

pubs.acs.org/JCTC Article

Relativistic Semistochastic Heat-Bath Configuration Interaction

Xubo Wang* and Sandeep Sharma*



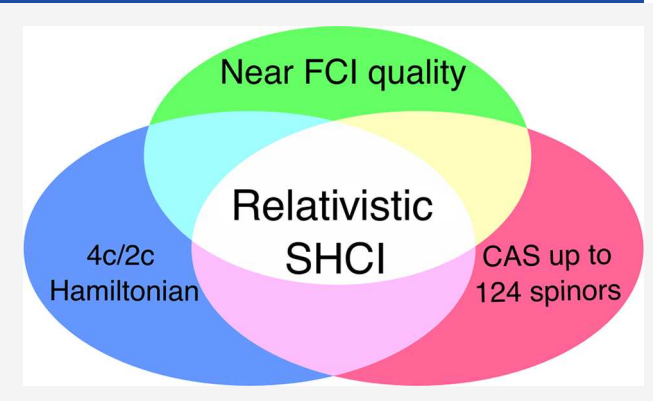
Cite This: J. Chem. Theory Comput. 2023, 19, 848-855



ACCESS I

Metrics & More

ABSTRACT: In this work we present the extension of semi-stochastic heat-bath configuration interaction (SHCI) to work with any two-component and four-component Hamiltonian. The vertical detachment energy (VDE) of AuH_2^- and zero-field splitting (ZFS) of NpO_2^{2+} is calculated by correlating more than 100 spinors in both cases. This work demonstrates the capability of SHCI to treat problems where both relativistic effect and electron correlation are important.



Article Recommendations

1. INTRODUCTION

The relativistic effect becomes more important as one goes down the Periodic Table¹⁻³ and gives rise to various phenomena, such as lanthanide contraction, mercury being liquid, simple cubic structure of polonium, etc. A proper relativistic Hamiltonian is needed to address these effects. In practice, the most rigorous relativistic Hamiltonian is the fourcomponent Dirac-Coulomb-Breit (DCB) Hamiltonian which reduces to the Dirac-Coulomb (DC) Hamiltonian when the Gaunt term and gauge term are omitted. 4,5 The four-component Hamiltonian supports the electron-positron pair-creation processes; however, such a process involves high energy (of the order of $2m_ec^2$ or 1.02 MeV)⁶ and thus does not play an important role in the chemical process. In light of this, various electron-only two-component Hamiltonians are derived to reduce the dimension of the problem, examples of which include the Zeroth Order Regular Approximation (ZORA),⁷ the Douglas-Kroll-Hess (DKH) Hamiltonian, 8,9 the Barysz-Sadlej-Snijders (BSS) Hamiltonian, 10 and exact two-component (X2C). 11-13 In X2C theory, the one electron operator is solved, and the transformation is then derived from the one electron solution in one step. The X2C transformation has therefore become popular due to its efficiency and accuracy.

Often, the one electron operator is chosen to be the oneelectron Dirac operator, and the two-electron term is simply the Coulomb operator. By doing so, the part of spin—orbit coupling (SOC) that originates from two-electron terms are completely neglected. One cost-effective way to treat the two-electron SOC terms is the spin—orbit mean field (SOMF) approach, where the relativistic two-body terms are treated approximately by including them in the Fock type one-body operator. In a SOMF calculation, one does a nonrelativistic or scalar relativistic

calculation, then computes the two electron SO integrals in the molecular orbitals obtained. The two electron SO integrals are then contracted with the spin-averaged self-consistent field (SCF) density matrix to obtain the effective one-electron SO integrals. But for heavy elements, the use of scalar orbital would cause noticeable errors, 16 and using spinors can give more accurate results since the molecular spinors are then fully relaxed under SOC. Such a molecular mean-field approach uses the density matrix and spinors from a four-component mean field wave function. ¹⁷ In this scheme, one first does a four-component mean field calculation, then block diagonalizes the so-obtained Fock matrix, the decoupling of the Fock matrix is just an X2C transformation of the Fock matrix, and is thus called X2CMMF¹⁷ (exact 2-component molecular mean field). One can avoid the cost of performing a full 4-component mean field calculation by exploiting the local nature of the SOC, and this strategy yields the atomic mean field (AMF) approach. 18-22 In AMF, an atomic SCF is performed and then the SO integral is contracted to the mean field form. The use of atomic integrals greatly reduced the cost and has been shown to be highly accurate. The AMF approach using 4c Hamiltonian to generate mean field SO integral²⁰ including even the Gaunt or Breit term has been proposed recently^{22,23} and is used in most calculations in this work.

Received: October 17, 2022 Published: January 26, 2023





During the past few decades, quantum chemistry algorithms that have been successful for nonrelativistic systems have also become available for 4c and 2c Hamiltonians, such as self-consistent field, density functional theory, coupled cluster, configuration interaction, and multiconfiguration self-consistent field, multireference perturbation theory (MRPT), multireference configuration interaction (MRCI), do, detail of the perform these relativistic electronic structure calculations.

In this work, we extend the semistochastic heat-bath configuration interaction (SHCI) algorithm⁵¹ to treat two- or four-component Hamiltonians with large active spaces. In our previous work⁵² to treat SOC using SHCI, we used scalar orbitals with SOMF integrals. This time we work with spinors which is expected to give a better description of SOC at the orbital optimization level. To our knowledge, only the density matrix renormalization group (DMRG)^{S3,S4} and full configuration interaction quantum Monte Carlo (FCIQMC)⁵⁵ have been implemented for 2c/4c Hamiltonians with the capability of treating around 100 molecular spinors; however, SHCI is often faster than both FCIQMC and DMRG for treating nonrelativistic Hamiltonians of molecules, and we expect this to be the case for relativistic Hamiltonians as well. 40 This paper is organized as follows. In section 2 and section 3, we describe the current SHCI algorithm, and the adaptation of SHCI algorithm to treat 2c/4c Hamiltonians including some implementation details. In section 4, we present the relativistic Hamiltonians we use in the calculations. In section 5, we give computational details and results on the vertical detachment energy (VDE) of AuH₂ and the first few excited states of NpO₂²⁺.

2. RECAP OF SHCI

Semistochastic heat-bath configuration interaction is a recently developed variant of the class of methods that perform a selected configuration interaction followed by perturbation theory (SCI-PT). Similar to all other SCI-PT methods, $^{56-59}$ it consists of a variational step and a perturbative step. In the variational step, a set of important determinants is iteratively selected by the heat-bath algorithm and the subspace eigenvalue problem is solved. In the perturbative step, the previously obtained variational energy is corrected by Epstein-Nesbet perturbation theory 60,61 to estimate the FCI energy. A semistochastic 51 scheme is utilized to reduce the cost. In this section, index i and a represent determinants inside or outside of the current variational space.

2.1. Heat-Bath Sampling. Given a set of initial determinants, the multi-reference wave function

$$|\Psi\rangle = \sum_{D_i \in \mathcal{V}} c_i |D_i\rangle \tag{1}$$

is obtained by diagonalizing the Hamiltonian in the current space ${\mathcal V}$ of important determinants. Then new determinants that satisfy the heat-bath criterion

$$\max_{D_i \in \mathcal{V}} |H_{ai}c_i| > \epsilon_1 \tag{2}$$

are added to the space \mathcal{V} . Here $H_{ai} = \langle D_a | \hat{H} | D_i \rangle$ is the Hamiltonian matrix element and ϵ_1 is a user defined parameter and is usually set to as small as possible. The HCI criterion is different from the one used in CIPSI, ⁵⁶ which is based on the contribution of a determinant D_a to the perturbative correction to the wave function

$$\frac{\sum_{|D_i\rangle \in \mathcal{V}} H_{ai} c_i}{E_0 - E_a} > \epsilon_1 \tag{3}$$

Although the HCI criterion is not optimal at picking out the important determinants, the variational space formed by the two methods is still nearly the same. Moreover, this *inexpensive to evaluate* selection criterion is implemented even more efficiently by avoiding generation of the determinants that do not meet the criterion, speeding up both variational and perturbative stages of the algorithm. For more detailed discussion on efficient implementation of SHCI, we refer the readers to previous works \$^{51,63}\$

2.2. Stochastic Perturbation Theory. After the variational stage, a perturbative step is performed to estimate the FCI energy by Epstein-Nesbet perturbation theory,

$$E_2 = \sum_{|D_a\rangle \in C} \frac{1}{E_0 - E_a} \left(\sum_{|D_i\rangle \in \mathcal{V}} H_{ai} c_i \right) \tag{4}$$

where C denotes the set of determinants that are connected to at least one determinant in \mathcal{V} by a nonzero Hamiltonian matrix element. Since the vast majority of terms in the double sum contribute negligibly, they can be discarded without significant loss of accuracy and the perturbative correction can be approximated by a "screened sum",

$$E_2(\epsilon_2) = \sum_{|D_a\rangle} \frac{1}{E_0 - E_a} \left(\sum_{i=1}^{(\epsilon_2)} H_{ai} c_i \right)$$
(5)

where $\sum^{\epsilon_2} H_{ai} c_i$ includes only terms with $|H_{ai} c_i| > \epsilon_2$ and the outer sum is over the determinants $|D_a\rangle$ that meet this criterion. In order to achieve good accuracy, this parameter ϵ_2 has to be small. Thus, even with a "screened sum", we might still encounter a memory bottleneck of having to store all the determinants $|D_a\rangle$ and their perturbative contribution in memory.

To further reduce the memory cost, we utilize the semistochastic perturbation theory to estimate the perturbative correction. In our semistochastic perturbation approach, a deterministic perturbative calculation with a relatively loose ϵ_2^d is performed first (termed as $E_2^D(\epsilon_2^d)$). The error caused by this loose parameter is then corrected stochastically by a much tighter ϵ_2 . In this step, a few tens to hundreds of variational determinants are sampled, and the perturbative correction is calculated using both ϵ_2^d and ϵ_2 (termed as $E_2^S(\epsilon_2)$ and $E_2^S(\epsilon_2^d)$), the final perturbation correction is estimated by

$$E_{2}(\epsilon_{2}) = E_{2}^{D}(\epsilon_{2}^{d}) + [E_{2}^{S}(\epsilon_{2}) - E_{2}^{S}(\epsilon_{2}^{d})]$$
 (6)

The key point to this scheme is that $E_2^S(\varepsilon_2)$ and $E_2^S(\varepsilon_2^d)$ are calculated using the exact same set of determinants and thus reduce the stochastic error significantly, with almost no increase in memory or computer time.

2.3. Excited States. With the four-component Hamiltonian being used, spin—orbit coupling and all other relativistic effects are taken into account naturally, thus $\langle S_z \rangle$ is no longer a good quantum number, the wave function becomes eigenfunction of the total angular momentum J. The 2S+1 fold degeneracy of a spin multiplet thus breaks into several sets of states corresponding to different J values with 2J+1 fold degeneracy. This energy splitting between different J states can be measured experimentally to determine the zero-field splitting (ZFS), and

they are usually very small compared to the absolute energies of the molecule.

In order to compute these excited states, the heat-bath criterion needs to be modified. It has been done in two different ways previously, ^{52,62} the first is to replace the ground state CI vector by the maximum values among all CI vectors

$$\max_{D_i \in \mathcal{V}} |H_{ai}| \max_{s \in \text{states}} |c_i^{(s)}| > \epsilon_1 \tag{7}$$

The second way is to use the averaged CI vector

$$\max_{D_i \in \mathcal{V}} \left| H_{ai} \frac{\sqrt{\sum_{s \in \text{states}} |c_i^s|^2}}{\text{no. of states}} \right| > \epsilon_1$$
(8)

As has been discussed before, 52 the second way is more appropriate for handling the small splitting and near degeneracy originating from the relativistic Hamiltonian. We thus use eq 8 as the heat-bath criterion for excited states calculations.

3. SHCI IN SPINOR BASIS

In this work, our relativistic SHCI implementation works on complex-valued spinor reference wave function, any 2c or 4c Hamiltonian that works in a spinor basis can readily be used. With the 2c/4c Hamiltonian being used, the spin symmetry and point group symmetry which are commonly used in non-relativistic calculations no longer hold, we instead have Kramer symmetry and double group symmetry that work for the four-component Hamiltonian. In the current implementation, we do not assume symmetry between barred and unbarred spinors, only permutation symmetry and complex-conjugated symmetry are utilized. Here, p, q, r, and s denote a general molecular spinor index.

$$(pq|rs) = (rs|pq) \tag{9}$$

$$(pq|rs) = (qp|sr)^* (10)$$

With the electron integrals being complex, the resulting Hamiltonian matrix at the variational stage is also a complex-valued Hermitian matrix, a complex version of the Davidson algorithm has been implemented in our previous work to solve the complex-valued eigenvalue problem. However, the heat-bath criterion in eq 2 and its variant for multiple roots in eq 8 as well as the perturbation correction in eq 4 are not influenced by the complex nature of the Hamiltonian since they both use the magnitude of $H_{ai}c_i$.

3.1. Implementation. Here we briefly describe the implementation and the steps of the leading order cost of the algorithm. There are three major operations during the variational stage: identify the important determinants, construct the Hamiltonian matrix, and diagonalize the matrix. In the current implementation, all the nonzero elements of the Hamiltonian are stored in memory using a list of lists (LIL) format. In the LIL format, we store a list of column indexes and a list of corresponding nonzero Hamiltonian matrix elements for a given determinant. The determinants are stored in a list of bitpacked strings that represent the occupation of the active molecular spinors. Since spin is no longer a good quantum number, the use of auxiliary lists implemented in the nonrelativistic case becomes complicated and more auxiliary lists are required. To simplify the problem, we noticed that if two determinants are connected by a single or double excitation,

then there exists a determinant with N-2 electrons occupied associated with both determinants. This idea can date back to Harrison et al.'s full configuration interaction (FCI) implementation⁶⁴ that is used in the relativistic FCI implementation by Bates et al.³⁷ We can further say that, if a set of determinants are associated with the same N-2 determinant, then they all have a nonzero Hamiltonian matrix element with each other according to the Slater-Condon rule. To make use of this fact, we generate a list of all the N-2 determinants, and then record all the Ndeterminants associated with each N-2 determinant. When constructing the Hamiltonian, we can make use of these two lists to help us find the connected determinants rather than searching the entire variation space. Also at each step, only the matrix elements associated with the newly added determinants are handled instead of constructing the Hamiltonian matrix from scratch every step.

Once the Hamiltonian is generated, a complex version of Davidson algorithm is used to obtain the lowest few eigenvalues where the most expensive step is Hamiltonian wave function multiplication which scales as $O(kN_V)$, where k is proportional to the fourth power of the number of electrons and is equal to the number of columns of the Hamiltonian matrix with nonzero values for a given determinant. The Hamiltonian matrix is currently stored in memory, and it is the largest bottleneck in a variational calculation.

The semistochastic perturbation scheme is identical to its nonrelativistic variant, for detailed discussion, we recommend readers follow previous work by one of the authors.

4. RELATIVISTIC HAMILTONIAN

4.1. 4c Hamiltonian. The four-component DC(B) Hamiltonian can be written as

$$\hat{H} = \sum_{i} \hat{h}_{D}(i) + \frac{1}{2} \sum_{i \neq j} \hat{g}(i, j) + V_{NN}$$
(11)

$$\hat{h}_{D}(i) = c^{2}(\beta - \mathbf{I}_{4}) + c(\boldsymbol{\alpha}_{i} \cdot \hat{\boldsymbol{p}}_{i}) - \sum_{A}^{\text{atoms}} \frac{Z_{A}}{r_{iA}}$$
(12)

$$\hat{g}(i,j) = \underbrace{\frac{1}{r_{ij}}}_{\text{Coulomb}} - \underbrace{\frac{\alpha_i \cdot \alpha_j}{r_{ij}}}_{\text{Gaunt}} + \underbrace{\frac{\alpha_i \cdot \alpha_j}{2r_{ij}} - \frac{(\alpha_i \cdot r_{ij})(\alpha_j \cdot r_{ij})}{2r_{ij}}}_{\text{gauge}}$$
Breit

where $\alpha = (\alpha_x, \alpha_y, \alpha_z)$, α_x , α_y , α_z and β are the 4 × 4 Dirac matrices

$$\alpha_{x} = \begin{pmatrix} \mathbf{0}_{2} & \sigma_{x} \\ \sigma_{x} & \mathbf{0}_{2} \end{pmatrix}, \quad \alpha_{y} = \begin{pmatrix} \mathbf{0}_{2} & \sigma_{y} \\ \sigma_{y} & \mathbf{0}_{2} \end{pmatrix}, \quad \alpha_{z} = \begin{pmatrix} \mathbf{0}_{2} & \sigma_{z} \\ \sigma_{z} & \mathbf{0}_{2} \end{pmatrix},$$

$$\beta = \begin{pmatrix} \mathbf{I}_{2} & \mathbf{0}_{2} \\ \mathbf{0}_{2} & -I_{2} \end{pmatrix} \tag{14}$$

 σ_{xy} σ_{yy} and σ_{z} are the Pauli matrices.

After the adoption of the no-pair approximation, the Hamiltonian in the second quantization form becomes

$$\hat{H} = \sum_{pq} h_{pq} \hat{a}_{p}^{\dagger} \hat{a}_{q} + \frac{1}{2} \sum_{pqrs} g_{pq,rs} \hat{a}_{p}^{\dagger} \hat{a}_{r}^{\dagger} \hat{a}_{s} \hat{a}_{q}$$
(15)

where the *p*, *q*, *r*, and *s* indices represent positive energy spinors. This no-pair Hamiltonian is what relativistic SHCI actually uses when doing a four-component correlation calculation.

4.2. X2CAMF Hamiltonian. In this work we use an X2CAMF Hamiltonian proposed by Liu et al.²⁰ to treat spinorbit coupling. In a standard X2C calculation, the bare Coulomb term is used as the two electron operator. The spin-dependent Coulomb interaction and the entire Breit term are then missing. To overcome this shortcoming the molecular mean field approach¹⁷ was previously proposed, whereby, a 4c Dirac Hartree-Fock calculation is performed on the entire molecule and then X2C transformation of the entire Fock matrix is carried out. All the non-Coulomb terms as well as the spin-orbit part of the Coulomb terms are absorbed into the one-body operator in a mean-field fashion. The disadvantage is that one still needs to do a molecular 4c calculation which is usually expensive. In the AMF approach, only atomic calculations are performed and then a separate X2C transformation for each atom is carried out. This approach relies on the local nature of the spin-orbit coupling. By doing the atomic calculation, one can also exploit the high symmetry in atoms which can greatly reduce the cost. A recent work by Zhang et al.²³ utilizes this feature and is implemented for the full DCB Hamiltonian.

AMF Hamiltonian. We start from the spin-separation scheme for the DC Hamiltonian to derive the atomic mean-field (AMF) Hamiltonian. The Coulomb operator can be partitioned into a spin-free part and a spin-dependent part.

$$g_{pq,rs}^{C} = g_{pq,rs}^{C,SF} + g_{pq,rs}^{C,SD}$$
 (16)

The full DCB Hamiltonian can thus be regrouped as

$$H^{\text{DCB}} = \sum_{pq} h_{pq} a_{p}^{\dagger} a_{q} + \frac{1}{2} \sum_{pqrs} (g_{pq,rs}^{\text{C,SD}} + g_{pq,rs}^{\text{Breit}}) \hat{a}_{p}^{\dagger} \hat{a}_{r}^{\dagger} \hat{a}_{s} \hat{a}_{q} + \frac{1}{2} \sum_{pqrs} g_{pq,rs}^{\text{C,SF}} \hat{a}_{p}^{\dagger} \hat{a}_{r}^{\dagger} \hat{a}_{s} \hat{a}_{q}$$

$$(17)$$

Although the Breit term can also be split into a spin-free term and spin-dependent term, ⁶⁵ it is still grouped together with the spin-dependent Coulomb term and treated within the atomic mean-field approximation. The atomic mean-field approximation is then introduced to treat the spin-dependent Coulomb and Breit terms

$$g_{pq}^{\text{AMF}} = \sum_{A} \sum_{i_A \in A} n_{i_A} (g_{p_{i_A}, q_{i_A}}^{\text{C,SD,A}} + g_{p_{i_A}, q_{i_A}}^{\text{Breit,A}} - g_{pq, i_A i_A}^{\text{C,SD,A}} - g_{pq, i_A i_A}^{\text{Breit,A}})$$
(18)

where the superscript A denotes the integral on each atom, i_A and n_{i_A} denote an occupied molecular orbital and the corresponding occupation number. The DCB Hamiltonian can then be approximated as

$$H^{\text{DCB,AMF}} \approx \sum_{pq} (h_{pq} + g_{pq}^{\text{AMF}}) \hat{a}_{p}^{\dagger} \hat{a}_{q} + \frac{1}{2} \sum_{ijkl} g_{pq,rs}^{\text{C,SF}} \hat{a}_{p}^{\dagger} \hat{a}_{r}^{\dagger} \hat{a}_{s} \hat{a}_{q}$$
(19)

X2C Transformation. Now we apply the standard X2C transformation 13 to this Hamiltonian. To derive the X2C transformation, one first replaces the small component (Ψ^S) with the pseudo-large-component (Φ^L)

$$\Psi^{S} = \frac{\sigma \cdot p}{2c} \Phi^{L} \tag{20}$$

The matrix Dirac equation can then be written in a modified form

$$\begin{pmatrix} \mathbf{V} & \mathbf{T} \\ \mathbf{T} & \frac{\alpha^2}{4} \mathbf{W} - \mathbf{T} \end{pmatrix} \begin{pmatrix} \mathbf{\Psi}^L \\ \mathbf{\Phi}^L \end{pmatrix} = \begin{pmatrix} \mathbf{S} & \mathbf{0} \\ \mathbf{0} & \frac{\alpha^2}{4} \mathbf{T} \end{pmatrix} \begin{pmatrix} \mathbf{\Psi}^L \\ \mathbf{\Phi}^L \end{pmatrix} \boldsymbol{\epsilon}$$
(21)

in which **V** is the potential matrix, **T** is the kinetic energy matrix, and **W** is the potential matrix for small components $(\boldsymbol{\sigma} \cdot \mathbf{p})V(\boldsymbol{\sigma} \cdot \mathbf{p})$.

In order to decouple the large and small component, a transformation matrix **U** that can block diagonalize the matrix equation is introduced

$$\mathbf{U} = \mathbf{U}_{N}\mathbf{U}_{D}, \quad \mathbf{U}_{N} = \begin{pmatrix} \mathbf{R}_{+}^{\dagger} & 0 \\ 0 & \mathbf{R}_{-}^{\dagger} \end{pmatrix}, \quad \mathbf{U}_{D} = \begin{pmatrix} \mathbf{I} & \mathbf{X}^{\dagger} \\ \tilde{\mathbf{X}}^{\dagger} & \mathbf{I} \end{pmatrix}$$
(22)

 \mathbf{U}_D achieves the decoupling and \mathbf{U}_N renormalizes the Hamiltonian to the nonrelativistic metric. The transformed matrix features a block diagonal form; electronic and positronic degrees of freedom are completely decoupled

$$\mathbf{U}\mathbf{h}_{D}\mathbf{U}^{\dagger} = \begin{pmatrix} \mathbf{h}_{D}^{+} & 0\\ 0 & \mathbf{h}_{D}^{-} \end{pmatrix} \tag{23}$$

To construct \mathbf{h}_D^+ , only \mathbf{R}^+ and \mathbf{X} is required, thus we introduce the \mathbf{X} matrix that relates $\mathbf{\Psi}^L$ and $\mathbf{\Phi}^L$

$$\Phi^{L} = \mathbf{X}\Phi^{L} \tag{24}$$

and the R^+ matrix that relates decoupled electronic wave function and the original large component wave function.

$$\Psi^L = \mathbf{R}^+ \Psi^+ \tag{25}$$

$$\mathbf{R}^{+} = (\mathbf{S}^{-1}\tilde{\mathbf{S}})^{-1/2}, \quad \tilde{\mathbf{S}} = \mathbf{S} + \frac{\alpha^{2}}{2}\mathbf{X}^{\dagger}\mathbf{T}\mathbf{X}$$
 (26)

The $\mathbf{h}_{\mathrm{D}}^{+}$ or the $\mathbf{h}_{\mathrm{X2C}}$ can be written as

$$\mathbf{h}_{X2C} = \mathbf{R}^{+\dagger} \{ \mathbf{h}_D^{LL} + \mathbf{X}^{\dagger} \mathbf{h}_D^{LS} + \mathbf{h}_D^{SL} \mathbf{X} + \mathbf{X}^{\dagger} (\mathbf{h}_D^{SS}) \mathbf{X} \} \mathbf{R}^{+}$$
 (27)

Note the above transformation only transforms the one-electron Dirac Hamiltonian, so we call it one-electron X2C Hamiltonian (\mathbf{h}^{X2C-1e}). The AMF term is transformed atomically. For each atom, a 4c calculation is performed, and the atomic Fock matrix takes the place of \mathbf{h}^D to determine the atomic X and R matrices. These atomic X and R matrices are then used to transform \mathbf{h}^{AMF} to $\mathbf{h}^{2c,AMF}$. The X2CAMF Hamiltonian²³ is then written as

$$\mathbf{H}^{\text{X2CAMF}} = \sum_{ij} (h_{ij}^{\text{X2C-1e}} + h_{ij}^{\text{2c,AMF}}) E_{ij} + \frac{1}{2} \sum_{ijkl} g_{ijkl}^{\text{NR}} E_{ijkl}$$
(28)

5. RESULTS

5.1. Computational Details. We present calculations to evaluate the photoelectron detachment energies (DE) of AuH₂⁻ which result in the formation of neutral open-shell molecule AuH₂ in different states. We also calculate the zero-field splitting (ZFS) of NpO₂²⁺. The X2CAMF Hamiltonian is computed using the X2CAMF package by Zhang. The X2CAMF Hartree–Fock (HF) calculations are performed through the socutils code by one of the authors. The SHCI calculations are performed using the ZSHCI module of the Dice code by the

authors.⁶⁸ The input and output for all calculations can be accessed from a public repository.⁶⁹ All the SHCI calculations use an ϵ_2 value of 10^{-10} a.u., and the stochastic errors are converged to 5×10^{-6} a.u. in order to recover the degeneracy between Kramer doublets. We extrapolate to the FCI limit by fitting the total energy $E_{\rm tot}=E_{\rm var}+E_2$ with respect to the PT2 correction E_2 .⁶² The extrapolation error is estimated to be one-fifth of the difference between the calculated energy with the smallest value of ϵ_1 .

5.2. Vertical Detachment Energy of AuH₂⁻. The photoelectron spectrum of AuH₂⁻ was accurately measured by Liu et al.⁷⁰ In the experiment work, the vibrational spectra of X state and A state are well resolved and were discussed carefully (Figure 1). The X state is the ground state of the AuH₂ and it has

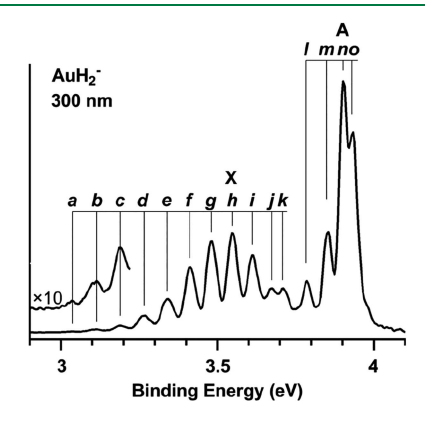


Figure 1. Vibrational resolved PES spectra for X state and A state from the experiments published in paper 70.

a bent geometry, peak "a" to peak "k" are considered to be the result of vibrational progression, the peak "a" corresponds to the adiabatic detachment energy (ADE), peak "h" with the highest intensity is deemed to be the vertical detachment energy (VDE). The spacing between these peaks (except for peak "k") can be fit well using the anharmonic vibrational model:

$$E_{\nu} = (\nu + 1/2)\omega_h - (\nu + 1/2)^2 \omega_h \chi_e \tag{29}$$

Peak "I" to peak "o" are assigned to be vibration levels of the A state, but the spacing between them do not fit into this model well. The authors proposed a slightly bent structure for A. More recent work by Sorbelli et al. 1 used X2C-EOM-CCSD to calculate the system and reinterpret the spectrum. They have proposed that state A has a linear structure, the unusual behavior in the peak "I" to "o" was explained as the pseudo-Jahn—Teller (PJTE) effect. They claimed that the PJTE induces a symmetry breaking along the asymmetric stretching coordinate, the

centrosymmetric linear nuclear configuration thus becomes a saddle point and the most stable configuration would be an asymmetric configuration. Here we calculated the vertical detachment energies (VDE) from the experimentally measured X band up to E band. The main focus in this work is not to give any new explanation to this spectroscopy problem but rather to have a comparison with the EOM-CCSD results especially when SHCI can give near exact results to see how they compare. The geometry ($r_{\rm Au-H}=1.647$ Å, $\alpha_{\rm H-Au-H}=180^{\circ}$) is taken from the experiment work. The X2CAMF-HF wave function for closed shell AuH₂ is used for both AuH₂ and AuH₂ calculation as the reference wave function.

The VDEs from X state up to E state using EOM-CCSD with both X2CAMF and X2CMMF Hamiltonian and SHCI with X2CAMF Hamiltonian under different active spaces are listed in Table 1. Both Hamiltonians contain relativistic effects up to the Gaunt term. The Dyall's triple- ζ basis set^{72,73} is used for all atoms based on results from a previous theory paper. One large EOM-CCSD calculation which correlates virtual spinors up to 100 hartree is also performed and is used to estimate the missing dynamic correlation in the SHCI calculation with 124 spinors correlated as shown in eq 30. The extrapolation error are within 0.007 eV for all 82 spinor calculations and 0.016 eV for 124 spinor calculations.

$$\mathbf{E}_{\text{composite}}^{\text{SHCI}} = \mathbf{E}_{\text{124spinors}}^{\text{SHCI}} - \mathbf{E}_{\text{124spinors}}^{\text{EOMCC}} + \mathbf{E}_{\text{100Hartree}}^{\text{EOMCC}}$$
(30)

We start by looking at the difference between X2CAMF and X2CMMF Hamiltonian from EOM-CCSD calculations at three different active spaces. The energy of X2CAMF is systematically lower by 1 meV than X2CMMF for state X and state A. For the other four states, the X2CAMF energy is higher than X2CMMF for around 4 meV. This difference between the two different Hamiltonians is consistent and also much smaller than other uncertainties in the calculations.

Then we may compare the EOM results and SHCI results with 82 spinors and 124 spinors active space. In the 82 spinors calculation, the X state and A state are misordered for both methods. If we compare the VDEs for state A to state E between the methods, we notice that the EOM-CCSD systematically underestimates them by 0.255 to 0.273 eV while it only underestimates the X state by 0.088 eV. When the larger active space with 124 spinors is used, the EOM-CCSD still underestimates the VDEs compared to the near-exact SHCI results, but the discrepancy reduces to within 0.130 to 0.156 eV. The VDE for the X state, however, behaves differently. The VDE from SHCI decreases while the EOM-CCSD VDE increases. While the composite SHCI energy gives a good agreement with experiment for the X state and A state, the VDE from the B state

Table 1. VDEs (in eV) of AuH₂ with 5d and 6s Electrons Correlated^a

	82 spinors			124 spinors			up to 100 hartree			
	EOM	EOM	SHCI	EOM	EOM	SHCI	EOM	EOM	SHCI	
State	MMF	AMF	AMF	MMF	AMF	AMF	MMF	AMF	(composite)	expt
X	3.517	3.516	3.604	3.545	3.544	3.521	3.666	3.665	3.641	3.678
A	3.292	3.292	3.560	3.627	3.626	3.744	3.792	3.791	3.909	3.904
В	4.019	4.023	4.296	4.499	4.504	4.653	4.740	4.745	4.895	4.635
C	4.123	4.127	4.398	4.582	4.587	4.741	4.834	4.838	4.992	4.785
D	5.128	5.131	5.372	5.510	5.513	5.643	5.768	5.771	5.902	5.745
E	5.600	5.604	5.859	6.007	6.011	6.167	6.275	6.280	6.435	6.220

^aThe EOM results underestimate energy of state A at all active spaces.

to E state are all overestimated while the reference EOM results achieve a better agreement with experiment values. This good agreement with experiments is likely caused by some fortuitous error cancellation. The composite VDE of X state and A state agrees with the experiment value better than the EOM-CCSD result. In particular, if one looks at the difference between energies of the X and the A states, the EOM-CCSD always gives a smaller gap between the two states since it underestimates the energy of the A state.

5.3. NpO₂²⁺. The rather stable actinyl ions, AnO₂ⁿ⁺, as well as their derivatives have interesting electronic structures and magnetic properties due to the similar order of SOC and crystal field effects and have therefore drawn people's attention. Previous work by Gendron et al. ^{74,75} has systematically studied the neptunyl ion NpO₂²⁺ and its derivative using multireference methods and includes SOC by means of state interaction. A state interaction version of DMRG⁷⁶ and our previous one-step SHCI treatment of SOC⁵² have been used to calculate the energies of the neptunyl ion. It is worth mentioning that all the previous calculations are based on different spin-free reference wave functions, and include the SOC terms at the correlation level.

We use the uncontracted ANO-RCC basis⁷⁸ for Np and the uncontracted cc-pVTZ basis⁷⁸ for O. The linear geometry with both Np–O bond lengths of 1.70 Å is taken from the work of Gendron et al.⁷⁴ A fraction occupation X2CAMF-HF is used as the reference state. The one open-shell electron is averaged in 4 spatial orbitals to give equal description on the four lowest Kramer doublets. The energies of the four doublets from this work as well some previous results are tabulated in Table 2. The

Table 2. Relative Energies (cm⁻¹) of the Electronic States of NpO₂²⁺ Calculated with X2CAMF Hamiltonian with the Breit Term Included for Two Different Active Spaces^a

		(current rork)	CASPT2- SO ⁷⁵	CASSCF- SO ⁷⁵	SO- SHCI ⁵²	
State	(40,1e)	(60o,13e)	(10o,7e)	(10o,7e)	(1430,17e)	
$^{2}\Phi_{5/2}$	0	0	0	0	0	
$^2\Delta_{3/2}$	3687	3429	3011	3179	3857	
$^{2}\Phi_{7/2}$	7640	7165	8092	8077	8675	
$^2\Delta_{5/2}$	9171	8868	9192	9288	10077	

 a All previous calculations using scalar relativistic orbitals underestimate the energy of the $^2\Delta_{3/2}$ state and overestimate the energy of the $^2\Phi_{7/2}$ state.

extrapolation error for all states are within 80 cm $^{-1}$. The spinor calculation gives different results than the previous spin—orbit calculations, where the splittings between $^2\Phi$ states and $^2\Delta$ states relative to the ground state are generally smaller. The difference can be attributed to the higher accuracy of the reference wave function in our present X2CAMF calculations where the orbital relaxation due to SOC is fully included, while in other calculations, SOC is only taken into account at the correlation level. Though the influence is generally not that large for lighter elements, Np is heavy enough so that the difference between the spinor reference and the scalar reference can be large.

6. CONCLUSIONS

We have extended the SHCI algorithm to treat general twocomponent Hamiltonian for both the ground and excited states. Our calculations show that SHCI is capable of treating the relativistic Hamiltonian with over 100 spinors. Application on VDEs of AuH_2 gives a better gap between the X state and A state which outperforms EOM-CCSD at the same basis set. The low energy spectrum of $NpO_2^{\ 2+}$ demonstrates that for such heavy elements, it is necessary to include relativistic effects at the SCF level.

The current method still has two limits, the variational Hamiltonian is very memory intensive because of the need to store the Hamiltonian and limits the variational space to a few million determinants. Thus, an efficient method to obtain the variational wave function is needed. A matrix-free eigensolver based on the coordinate descent algorithm is in development. Due to the number of electrons and large basis used in a relativistic calculation, even SHCI cannot treat a sufficient number of orbitals in the active space to account for dynamical correlation. Work in this direction is underway, we are working on a relativistic phaseless auxiliary field quantum Monte Carlo SO,81 with the relativistic HCI wave function as the trial state.

AUTHOR INFORMATION

Corresponding Authors

Xubo Wang – Department of Chemistry, University of Colorado Boulder, Boulder, Colorado 80309, United States;

orcid.org/0000-0003-3522-7435; Email: xubo.wang@colorado.edu

Sandeep Sharma — Department of Chemistry, University of Colorado Boulder, Boulder, Colorado 80309, United States; orcid.org/0000-0002-6598-8887;

Email: sandeep.sharma@colorado.edu

Complete contact information is available at: https://pubs.acs.org/10.1021/acs.jctc.2c01025

Notes

The authors declare no competing financial interest.

ACKNOWLEDGMENTS

X.W. was supported through the National Science Foundation grant CHE-2145209. S.S. was supported by the grant from the Camille and Henry Dreyfus foundation. All calculations were performed on the Blanca and Summit clusters at CU Boulder. We would also like to thank Chaoqun Zhang for discussion on the X2CAMF approach.

■ REFERENCES

- (1) Pyykkö, P. The Physics behind Chemistry and the Periodic Table. *Chem. Rev.* **2012**, *112*, *371*.
- (2) Pyykkö, P. Relativistic Effects in Chemistry: More Common Than You Thought. *Annu. Rev. Phys. Chem.* **2012**, *63*, 45–64.
- (3) Autschbach, J. Perspective: Relativistic Effects. J. Chem. Phys. 2012, 136, 150902.
- (4) Dyall, K. G.; Fægri, K.Introduction to Relativistic Quantum Chemistry; Oxford University Press, 2007.
- (5) Reiher, M.; Wolf, A.Relativistic Quantum Chemistry: The Fundamental Theory of Molecular Science; John Wiley & Sons, 2014.
- (6) Liu, W. Ideas of Relativistic Quantum Chemistry. Mol. Phys. 2010, 108, 1679.
- (7) van Lenthe, E.; Baerends, E. J.; Snijders, J. G. Relativistic Regular Two-component Hamiltonians. *J. Chem. Phys.* **1993**, *99*, 4597–4610.
- (8) Douglas, M.; Kroll, N. M. Quantum Electrodynamical Corrections to the Fine Structure of Helium. *Annals of Physics* **1974**, *82*, 89–155.
- (9) Hess, B. A. Relativistic Electronic-Structure Calculations Employing a Two-Component No-Pair Formalism with External-Field Projection Operators. *Phys. Rev. A* **1986**, *33*, 3742–3748.

- (10) Barysz, M.; Sadlej, A. J. Infinite-Order Two-Component Theory for Relativistic Quantum Chemistry. *J. Chem. Phys.* **2002**, *116*, 2696–2704.
- (11) Kutzelnigg, W.; Liu, W. Quasirelativistic Theory Equivalent to Fully Relativistic Theory. *J. Chem. Phys.* **2005**, *123*, 241102.
- (12) Iliaš, M.; Saue, T. An Infinite-Order Two-Component Relativistic Hamiltonian by a Simple One-Step Transformation. *J. Chem. Phys.* **2007**, *126*, 064102.
- (13) Liu, W.; Peng, D. Exact Two-Component Hamiltonians Revisited. J. Chem. Phys. 2009, 131, 1-5.
- (14) Heß, B. A.; Marian, C. M.; Wahlgren, U.; Gropen, O. A Mean-Field Spin-Orbit Method Applicable to Correlated Wavefunctions. *Chem. Phys. Lett.* **1996**, 251, 365–371.
- (15) Marian, C. M.; Wahlgren, U. A New Mean-Field and ECP-based Spin-Orbit Method. Applications to Pt and PtH. *Chem. Phys. Lett.* **1996**, 251, 357–364.
- (16) Iliaš, M.; Kellö, V.; Visscher, L.; Schimmelpfennig, B. Inclusion of Mean-Field Spin—Orbit Effects Based on All-Electron Two-Component Spinors: Pilot Calculations on Atomic and Molecular Properties. *J. Chem. Phys.* **2001**, *115*, 9667—9674.
- (17) Sikkema, J.; Visscher, L.; Saue, T.; Iliaš, M. The Molecular Mean-Field Approach for Correlated Relativistic Calculations. *J. Chem. Phys.* **2009**, *131*, 124116.
- (18) Schimmelpfennig, B.AMFI, an Atomic Mean-Field Spin-Orbit Integral Program; Bernd Schimmelpfennig: University of Stockholm, 1996.
- (19) Li, Z.; Xiao, Y.; Liu, W. On the Spin Separation of Algebraic Two-Component Relativistic Hamiltonians. *J. Chem. Phys.* **2012**, *137*, 154114.
- (20) Liu, J.; Cheng, L. An Atomic Mean-Field Spin-Orbit Approach within Exact Two-Component Theory for a Non-Perturbative Treatment of Spin-Orbit Coupling. *J. Chem. Phys.* **2018**, *148*, 144108.
- (21) Zhang, C.; Cheng, L. Performance of an Atomic Mean-Field Spin—Orbit Approach within Exact Two-Component Theory for Perturbative Treatment of Spin—Orbit Coupling. *Mol. Phys.* **2020**, *118*, No. e1768313.
- (22) Knecht, S.; Repisky, M.; Jensen, H. J. A.; Saue, T. Exact Two-Component Hamiltonians for Relativistic Quantum Chemistry: Two-electron Picture-Change Corrections Made Simple. *J. Chem. Phys.* **2022**, *157*, 114106.
- (23) Zhang, C.; Cheng, L. Atomic Mean-Field Approach within Exact Two-Component Theory Based on the Dirac—Coulomb—Breit Hamiltonian. *J. Phys. Chem. A* **2022**, *126*, 4537—4553.
- (24) Saue, T.; Jensen, H. J. A. Quaternion Symmetry in Relativistic Molecular Calculations: The Dirac-Hartree-Fock Method. *J. Chem. Phys.* **1999**, *111*, 6211–6222.
- (25) Anderson, J.; Sundahl, B.; Harrison, R.; Beylkin, G. Dirac-Fock Calculations on Molecules in an Adaptive Multiwavelet Basis. *J. Chem. Phys.* **2019**, *151*, 160901.
- (26) Liu, W.; Hong, G.; Dai, D.; Li, L.; Dolg, M. The Beijing Four-Component Density Functional Program Package (BDF) and Its Application to EuO, EuS, YbO and YbS. *Theor. Chem. Acc.* **1997**, *96*, 75–83.
- (27) Saue, T.; Helgaker, T. Four-Component Relativistic Kohn-Sham Theory. *J. Comput. Chem.* **2002**, 23, 814–823.
- (28) Visscher, L.; Eliav, E.; Kaldor, U. Formulation and Implementation of the Relativistic Fock-space Coupled Cluster Method for Molecules. *J. Chem. Phys.* **2001**, *115*, 9720–9726.
- (29) Nataraj, H. S.; Kállay, M.; Visscher, L. General Implementation of the Relativistic Coupled-Cluster Method. *J. Chem. Phys.* **2010**, *133*, 234109.
- (30) Asthana, A.; Liu, J.; Cheng, L. Exact Two-Component Equation-of-Motion Coupled-Cluster Singles and Doubles Method Using Atomic Mean-Field Spin-Orbit Integrals. *J. Chem. Phys.* **2019**, *150*, 074102
- (31) Cheng, L. A. Study of Non-Iterative Triples Contributions in Relativistic Equation-of-Motion Coupled-Cluster Calculations Using an Exact Two-Component Hamiltonian with Atomic Mean-Field Spin-

- Orbit Integrals: Application to Uranyl and Other Heavy-Element Compounds. J. Chem. Phys. 2019, 151, 104103.
- (32) Liu, J.; Cheng, L. Relativistic Coupled-Cluster and Equation-of-Motion Coupled-Cluster Methods. WIREs Computational Molecular Science 2021, 11, No. e1536.
- (33) Fleig, T.; Olsen, J.; Marian, C. M. The Generalized Active Space Concept for the Relativistic Treatment of Electron Correlation. I. Kramers-restricted Two-Component Configuration Interaction. *J. Chem. Phys.* **2001**, *114*, 4775–4790.
- (34) Knecht, S.; Jensen, H. J. A.; Fleig, T. Large-Scale Parallel Configuration Interaction. II. Two- and Four-Component Double-Group General Active Space Implementation with Application to BiH. *J. Chem. Phys.* **2010**, *132*, 014108.
- (35) Jo/rgen Aa. Jensen, H.; Dyall, K. G.; Saue, T.; Fægri, K. Relativistic Four-component Multiconfigurational Self-consistent-field Theory for Molecules: Formalism. *J. Chem. Phys.* **1996**, *104*, 4083–4097
- (36) Thyssen, J.; Fleig, T.; Jensen, H. J. A. A Direct Relativistic Four-Component Multiconfiguration Self-Consistent-Field Method for Molecules. *J. Chem. Phys.* **2008**, *129*, 104106.
- (37) Bates, J. E.; Shiozaki, T. Fully Relativistic Complete Active Space Self-Consistent Field for Large Molecules: Quasi-second-order Minimax Optimization. *J. Chem. Phys.* **2015**, *142*, 044112.
- (38) Reynolds, R. D.; Yanai, T.; Shiozaki, T. Large-Scale Relativistic Complete Active Space Self-Consistent Field with Robust Convergence. *J. Chem. Phys.* **2018**, *149*, 014106.
- (39) Jenkins, A. J.; Liu, H.; Kasper, J. M.; Frisch, M. J.; Li, X. Variational Relativistic Two-Component Complete-Active-Space Self-Consistent Field Method. *J. Chem. Theory Comput.* **2019**, *15*, 2974–2982.
- (40) Shiozaki, T.; Mizukami, W. Relativistic Internally Contracted Multireference Electron Correlation Methods. *J. Chem. Theory Comput.* **2015**, *11*, 4733–4739.
- (41) Lu, L.; Hu, H.; Jenkins, A. J.; Li, X. Exact-Two-Component Relativistic Multireference Second-Order Perturbation Theory. *J. Chem. Theory Comput.* **2022**, *18*, 2983–2992.
- (42) Hu, H.; Jenkins, A. J.; Liu, H.; Kasper, J. M.; Frisch, M. J.; Li, X. Relativistic Two-Component Multireference Configuration Interaction Method with Tunable Correlation Space. *J. Chem. Theory Comput.* **2020**, *16*, 2975–2984.
- (43) Jönsson, P.; Gaigalas, G.; Bieroń, J.; Fischer, C. F.; Grant, I. P. New Version: Grasp2K Relativistic Atomic Structure Package. *Comput. Phys. Commun.* **2013**, *184*, 2197–2203.
- (44) Saue, T.; Bast, R.; Gomes, A. S. P.; Jensen, H. J. A.; Visscher, L.; Aucar, I. A.; Di Remigio, R.; Dyall, K. G.; Eliav, E.; Fasshauer, E.; Fleig, T.; Halbert, L.; Hedegård, E. D.; Helmich-Paris, B.; Iliaš, M.; Jacob, C. R.; Knecht, S.; Laerdahl, J. K.; Vidal, M. L.; Nayak, M. K.; Olejniczak, M.; Olsen, J. M. H.; Pernpointner, M.; Senjean, B.; Shee, A.; Sunaga, A.; van Stralen, J. N. P. The DIRAC Code for Relativistic Molecular Calculations. *J. Chem. Phys.* **2020**, *152*, 204104.
- (45) Sun, Q.; Zhang, X.; Banerjee, S.; Bao, P.; Barbry, M.; Blunt, N. S.; Bogdanov, N. A.; Booth, G. H.; Chen, J.; Cui, Z.-H.; Eriksen, J. J.; Gao, Y.; Guo, S.; Hermann, J.; Hermes, M. R.; Koh, K.; Koval, P.; Lehtola, S.; Li, Z.; Liu, J.; Mardirossian, N.; McClain, J. D.; Motta, M.; Mussard, B.; Pham, H. Q.; Pulkin, A.; Purwanto, W.; Robinson, P. J.; Ronca, E.; Sayfutyarova, E. R.; Scheurer, M.; Schurkus, H. F.; Smith, J. E. T.; Sun, C.; Sun, S.-N.; Upadhyay, S.; Wagner, L. K.; Wang, X.; White, A.; Whitfield, J. D.; Williamson, M. J.; Wouters, S.; Yang, J.; Yu, J. M.; Zhu, T.; Berkelbach, T. C.; Sharma, S.; Sokolov, A. Y.; Chan, G. K.-L. Recent Developments in the PySCF Program Package. *J. Chem. Phys.* 2020, 153, 024109.
- (46) Shiozaki, T. BAGEL: Brilliantly Advanced General Electronic-structure Library. *Wiley Interdiscip. Rev. Comput. Mol. Sci.* **2018**, 8, No. e1331.
- (47) Williams-Young, D. B.; Petrone, A.; Sun, S.; Stetina, T. F.; Lestrange, P.; Hoyer, C. E.; Nascimento, D. R.; Koulias, L.; Wildman, A.; Kasper, J.; Goings, J. J.; Ding, F.; DePrince, A. E.; Valeev, E. F.; Li, X. The Chronus Quantum Software Package. WIREs Computational Molecular Science 2020, 10, 10.

- (48) Matthews, D. A.; Cheng, L.; Harding, M. E.; Lipparini, F.; Stopkowicz, S.; Jagau, T.-C.; Szalay, P. G.; Gauss, J.; Stanton, J. F. Coupled-Cluster Techniques for Computational Chemistry: The CFOUR Program Package. *J. Chem. Phys.* **2020**, *152*, 214108.
- (49) Belpassi, L.; De Santis, M.; Quiney, H. M.; Tarantelli, F.; Storchi, L. BERTHA: Implementation of a Four-Component Dirac–Kohn–Sham Relativistic Framework. *J. Chem. Phys.* **2020**, *152*, 164118.
- (50) Zhang, Y.; Suo, B.; Wang, Z.; Zhang, N.; Li, Z.; Lei, Y.; Zou, W.; Gao, J.; Peng, D.; Pu, Z.; Xiao, Y.; Sun, Q.; Wang, F.; Ma, Y.; Wang, X.; Guo, Y.; Liu, W. BDF: A Relativistic Electronic Structure Program Package. J. Chem. Phys. 2020, 152, 064113.
- (51) Sharma, S.; Holmes, A. A.; Jeanmairet, G.; Alavi, A.; Umrigar, C. J. Semistochastic Heat-bath Configuration Interaction Method: Selected Configuration Interaction with Semistochastic Perturbation Theory. J. Chem. Theory Comput. 2017, 13, 1595–1604.
- (52) Mussard, B.; Sharma, S. One-Step Treatment of Spin-Orbit Coupling and Electron Correlation in Large Active Spaces. *J. Chem. Theory Comput.* **2018**, *14*, 154–165.
- (53) Knecht, S.; Legeza, Ö.; Reiher, M. Communication: Four-component Density Matrix Renormalization Group. *J. Chem. Phys.* **2014**, *140*, 041101.
- (54) Battaglia, S.; Keller, S.; Knecht, S. Efficient Relativistic Density-Matrix Renormalization Group Implementation in a Matrix-Product Formulation. *J. Chem. Theory Comput.* **2018**, *14*, 2353–2369.
- (55) Anderson, R. J.; Booth, G. H. Four-Component Full Configuration Interaction Quantum Monte Carlo for Relativistic Correlated Electron Problems. *J. Chem. Phys.* **2020**, *153*, 184103.
- (56) Evangelisti, S.; Daudey, J.-P.; Malrieu, J.-P. Convergence of an Improved CIPSI Algorithm. *Chem. Phys.* **1983**, 75, 91–102.
- (57) Liu, W.; Hoffmann, M. R. iCI: Iterative CI toward Full CI. J. Chem. Theory Comput 2016, 12, 1169.
- (58) Schriber, J. B.; Evangelista, F. A. Communication: An Adaptive Configuration Interaction Approach for Strongly Correlated Electrons with Tunable Accuracy. *J. Chem. Phys.* **2016**, *144*, 161106.
- (59) Tubman, N. M.; Freeman, C. D.; Levine, D. S.; Hait, D.; Head-Gordon, M.; Whaley, K. B. Modern Approaches to Exact Diagonalization and Selected Configuration Interaction with the Adaptive Sampling CI Method. *J. Chem. Theory Comput.* **2020**, *16*, 2139–2159.
- (60) Epstein, P. S. The Stark Effect from the Point of View of Schroedinger's Quantum Theory. *Phys. Rev.* **1926**, 28, 6956.
- (61) Nesbet, R. K. Configuration Interaction in Orbital Theories. *Proc. R. Soc. London, Ser. A* **1955**, 230, 312.
- (62) Holmes, A. A.; Umrigar, C. J.; Sharma, S. Excited States Using Semistochastic Heat-Bath Configuration Interaction. *J. Chem. Phys.* **2017**, *147*, 164111.
- (63) Li, J.; Otten, M.; Holmes, A. A.; Sharma, S.; Umrigar, C. J. Fast Semistochastic Heat-Bath Configuration Interaction. *J. Chem. Phys.* **2018**, *149*, 214110.
- (64) Harrison, R. J.; Zarrabian, S. An Efficient Implementation of the Full-CI Method Using an (n-2)-Electron Projection Space. *Chem. Phys. Lett.* **1989**, *158*, 393–398.
- (65) Dyall, K. G. An Exact Separation of the Spin-free and Spin-dependent Terms of the Dirac—Coulomb—Breit Hamiltonian. *J. Chem. Phys.* **1994**, *100*, 2118—2127.
- (66) Zhang, C.x2camf; github, 2022. https://github.com/warlocat/x2camf.
- (67) Wang, X.Xubwa/Socutils; github, 2022. https://github.com/xubwa/socutils
- (68) Sharma, S.Dice; github, 2022. https://github.om/sanshar/Dice
- (69) Wang, X.Xubwa/RelHCI.; github, 2022. https://github.com/xubwa/RelHCI respectively.
- (70) Liu, H.-T.; Wang, Y.-L.; Xiong, X.-G.; Dau, P. D.; Piazza, Z. A.; Huang, D.-L.; Xu, C.-Q.; Li, J.; Wang, L.-S. The Electronic Structure and Chemical Bonding in Gold Dihydride: AuH 2 and AuH 2. *Chemical Science* **2012**, *3*, 3286–3295.
- (71) Sorbelli, D.; Belanzoni, P.; Saue, T.; Belpassi, L. Ground and Excited Electronic States of AuH ₂*via* Detachment Energies on AuH ₂⁻ Using State-of-the-Art Relativistic Calculations. *Phys. Chem. Chem. Phys.* **2020**, 22, 26742–26752.

- (72) Dyall, K. G.; Gomes, A. S. P. Revised Relativistic Basis Sets for the 5d Elements Hf–Hg. *Theor. Chem. Acc.* **2010**, *125*, 97.
- (73) Dyall, K. G. Relativistic Double-Zeta, Triple-Zeta, and Quadruple-Zeta Basis Sets for the Light Elements H-Ar. *Theor. Chem. Acc.* **2016**, *135*, 128.
- (74) Gendron, F.; Páez-Hernández, D.; Notter, F.-P.; Pritchard, B.; Bolvin, H.; Autschbach, J. Magnetic Properties and Electronic Structure of Neptunyl(VI) Complexes: Wavefunctions, Orbitals, and Crystal-Field Models. *Chem. A Eur. J.* **2014**, *20*, 7994–8011.
- (75) Gendron, F.; Pritchard, B.; Bolvin, H.; Autschbach, J. Magnetic Resonance Properties of Actinyl Carbonate Complexes and Plutonyl-(VI)-Tris-Nitrate. *Inorg. Chem.* **2014**, *53*, 8577–8592.
- (76) Knecht, S.; Keller, S.; Autschbach, J.; Reiher, M. A Non-orthogonal State-Interaction Approach for Matrix Product State Wave Functions. *J. Chem. Theory Comput.* **2016**, *12*, 5881–5894.
- (77) Roos, B. O.; Lindh, R.; Malmqvist, P.-Å.; Veryazov, V.; Widmark, P.-O. New Relativistic ANO Basis Sets for Transition Metal Atoms. *J. Phys. Chem. A* **2005**, *109*, 6575–6579.
- (78) Dunning, T. H.; Dunning, T. H., Jr Gaussian Basis Sets for Use in Correlated Molecular Calculations. I. The Atoms Boron through Neon and Hydrogen. *J. Chem. Phys.* **1989**, *90*, 1007–1023.
- (79) Wang, Z.; Li, Y.; Lu, J. Coordinate Descent Full Configuration Interaction. *J. Chem. Theory Comput.* **2019**, *15*, 3558–3569.
- (80) Motta, M.; Zhang, S. Ab Initio Computations of Molecular Systems by the Auxiliary-Field Quantum Monte Carlo Method. *WIREs Computational Molecular Science* **2018**, 8, No. e1364.
- (81) Eskridge, B.; Krakauer, H.; Shi, H.; Zhang, S. Ab Initio Calculations in Atoms, Molecules, and Solids, Treating Spin—Orbit Coupling and Electron Interaction on an Equal Footing. *J. Chem. Phys.* **2022**, *156*, 014107.
- (82) Mahajan, A.; Lee, J.; Sharma, S. Selected Configuration Interaction Wave Functions in Phaseless Auxiliary Field Quantum Monte Carlo. *J. Chem. Phys.* **2022**, *156*, 174111.

TRecommended by ACS

Orthogonally Constrained Orbital Optimization: Assessing Changes of Optimal Orbitals for Orthogonal Multireference States

Saad Yalouz and Vincent Robert

FEBRUARY 15, 2023

JOURNAL OF CHEMICAL THEORY AND COMPUTATION

READ 🗹

Analytical Formulation of the Second-Order Derivative of Energy for the Orbital-Optimized Variational Quantum Eigensolver: Application to Polarizability

Yuya O. Nakagawa, Wataru Mizukami, et al.

MARCH 28, 2023

JOURNAL OF CHEMICAL THEORY AND COMPUTATION

READ 🗹

Tensor Hypercontraction Form of the Perturbative Triples Energy in Coupled-Cluster Theory

Andy Jiang, Henry F. Schaefer III, et al.

FEBRUARY 17, 2023

JOURNAL OF CHEMICAL THEORY AND COMPUTATION

READ 🗹

Symmetrization of Localized Molecular Orbitals

Jonas Greiner and Janus J. Eriksen

APRIL 11, 2023

THE JOURNAL OF PHYSICAL CHEMISTRY A

READ 🗹

Get More Suggestions >